Precision Engineering xxx (2016) xxx–xxx

Contents lists available at ScienceDirect

Precision Engineering

journal homepage: www.elsevier.com/locate/precision

Large displacement behavior of double parallelogram flexure mechanisms with underconstraint eliminators

Robert M. Panas

Lawrence Livermore National Laboratory, L-229, 7000 East Avenue, Livermore, CA 94550, United States

ARTICLE INFO

Article history:
Received 19 August 2015
Received in revised form 3 March 2016
Accepted 21 June 2016
Available online xxx

Keywords:
Underconstraint elimination
Four-bar flexure
Folded flexure
Double parallelogram flexure
Nested linkage
Nonlinear beam analysis
Elastokinematic effect
Large displacement axial stiffness
Large stroke
Flexure mechanism

ABSTRACT

This paper presents a new analytical method for predicting the large displacement behavior of flexural double parallelogram (DP) bearings with underconstraint eliminator (UE) linkages. This closed-form perturbative Euler analysis method is able to – for the first time – directly incorporate the elastomechanics of a discrete UE linkage, which is a hybrid flexure element that is linked to ground as well as both stages on the bearing. The models are used to understand a nested linkage UE design, however the method is extensible to other UE linkages. Design rules and figures-of-merit are extracted from the analysis models, which provide powerful tools for accelerating the design process. The models, rules and figures-of-merit enable the rapid design of a UE for a desired large displacement behavior, as well as providing a means for determining the limits of UE and DP structures. This will aid in the adoption of UE linkages into DP bearings for precision mechanisms. Models are generated for a nested linkage UE design, and the performance of this DP with UE structure is compared to a DP-only bearing. The perturbative Euler analysis is shown to match existing theories for DP-only bearings with distributed compliance within ≈2%, and Finite Element Analysis for the DP with UE bearings within an average 10%.

1. Introduction

The intent of this work is to model the effect of a nested linkage underconstraint eliminator [1] on the large displacement y-axis stiffness of a flexural double parallelogram linear bearing. A new method is presented for the closed-form analysis of the large displacement axial stiffness which can easily incorporate the complex elastomechanics of a UE linkage, unlike existing large displacement models [2–18]. Design rules and new figures-of-merit are defined to further simplify the design process. These tools are demonstrated on a nested-linkage UE design as presented in [1], but they are generalizable to other UE designs. These tools enable the rapid, direct design of the UE for the desired large displacement behavior, in addition to mapping the performance limitations intrinsic to the DP bearing as well as those of the UE. This work will accelerate the adoption of UE linkages into DP bearings, as designers can now quickly analyze the tradeoffs associated with their use, even for large displacement applications. This offers the potential for improving bearing performance via reduced error motion, improved dynamics and greater bearing stiffness for a range of applications including their use as MEMS [5,6,19–27], single-/multi-axis precision positioning stages [19,28–32], and macroscale bearings [8,33–35].

1.1. Double parallelogram flexure bearing

Double parallelogram flexure bearings, as shown in Fig. 1, are commonly used in precision devices [8,13,18,34,36,37] for several reasons. The flexure component of the bearing can provide motion with very fine resolution, no stiction, and high repeatability [8,34] among other features. The double parallelogram structure provides increased range and reduced kinematic errors for its main translation Degree-of-Freedom (DOF) over that of a single parallelogram flexure bearing [2,18]. The kinematic errors of the single parallelogram are shown as elliptical arcs in Fig. 1b. At large displacements, these arcs begin to show a y-axis component. The second stage of the bearing shows these same errors in reverse, so the net effect is to cancel out the kinematic error at the final stage [2,18] given that the final and intermediate stages are allowed to move in a 2:1 ratio. This is shown in Fig. 1b with solid arrows.

The intermediate stage possesses the same translational DOF as the final stage [1,2,8,18,28,37,38]. The underconstraint is observable in two forms [1,18]. The freedom of the intermediate stage to vibrate appears as a relatively low frequency collocated

E-mail address: panas3@llnl.gov

http://dx.doi.org/10.1016/j.precisioneng.2016.06.010
0141-6359/

Nomenclature

Motion

θ_{ld}	Angle of flexures at large displacement (rad)
x_b	Transverse displacement of individual flexure blade (m)
x_f	X-axis displacement of final stage (m)
δ_{xi}	X-axis perturbation displacement of intermediate stage (m)
δ_{xf}	X-axis perturbation displacement of final stage (m)
δ_{yi}	Y-axis perturbation displacement of intermediate stage (m)
δ_{yf}	Y-axis perturbation displacement of final stage (m)
δ_{mt}	Transverse displacement of the type m flexure in the flexure reference frame (m)
δ_{ma}	Axial displacement of the type m flexure in the flexure reference frame (m)
X	X-axis displacement of final stage, nondimensionalized via hm

Large Displacement Effect Scale Figure-of-Merit

τ_b	LDES of single beam transverse motion
τ_{DP}	LDES of DP bearing with no UE main DOF
τ_{11}	LDES of type 11 flexures in main DOF
τ_{12}	LDES of type 12 flexures in main DOF
τ_2	LDES of type 2 flexures in main DOF
τ_m	LDES of type m flexures in main DOF
τ_{yf}	LDES of final stage y-axis elastokinematics
τ_{d2}	LDES of 1st order term, DP + UE net effect
τ_{d4}	LDES of 2nd order term, DP + UE net effect
τ_{nUE}	LDES of final stage y-axis net effect
τ_{nDP}	LDES of final stage y-axis net effect

Geometry

E	Young's modulus for all flexure types (Pa)
A	Axial-normal cross-sectional area for all flexure types (m^2)
I	Axial-normal second moment of area for all flexure types (m^4)
L	Length for all flexure types (m)
h	Bending direction thickness for all flexures (m)
γ	PRBM flexure length fraction
θ_2	Angle of type 2 flexures off the y-axis (rad)
r_1	Lever arm for type 1 flexures (m)
r_2	Lever arm for type 2 flexures (m)
d	Lever arm for UE rotation (m)
d_3	Separation between serial type m flexures (m)
a_0	Compliance distribution ratio

Forces

F_{mt}	Transverse reaction force of type m flexure (N)
F_{ma}	Axial reaction force of type m flexure (N)
F_{mx}	X-axis reaction force of type m flexure (N)
F_{my}	Y-axis reaction force of type m flexure (N)
F_x	X-axis reaction force to hold final stage (N)
F_y	Y-axis applied load on final stage (N)

Stiffness

k_{ma}	Axial stiffness for type m flexures (N/m)
k_{mt}	Transverse (in-plane) stiffness for type m flexures (N/m)
k_{pa}	Axial stiffness for type p flexures (N/m)
k_{pb}	Rigid body relaxation stiffness for type p flexures (N/m)

Stiffness

$k_{j\theta}$	Clamped-free z-axis moment-to-rotation stiffness for type j flexures (N-m /rad)
k_{jt}	Clamped-guided in-plane transverse force to displacement stiffness for type j flexures (N/m)
$k_{jt\tau}$	Clamped-free z-axis moment to in-plane transverse displacement stiffness (N-m/m)
k_{iue}	UE stiffness for intermediate stage underconstrained DOF motion (N/m)
k_{fue}	UE stiffness for final stage main translational DOF motion (N/m)
k_{ba}	Axial stiffness of a single beam (N/m)
k_{bae}	Euler axial stiffness of a single beam (N/m)
k_{DP}	Axial (y-axis) stiffness of a DP bearing with no UE (N/m)
k_{yi}	Y-axis stiffness for intermediate stage deformation (N/m)
k_{yf}	Y-axis stiffness for final stage (N/m)
r_k	Underconstrained DOF Stiffness ratio

Subscripts

m	Index for type m flexures
1	Index for type 1 flexures
11	Index for type 11 flexures
12	Index for type 12 flexures
2	Index for type 2 flexures
p	Index for type {11, 12, 2} flexures
j	Index for type {1, 2} flexures

resonance which can negatively affect the dynamics and control of the bearing [1,18]. Axial loading (y-axis) on the final stage at large displacements drives the intermediate stage back along its arcuate path towards equilibrium, while the flexures holding the final stage are further deflected, as shown in Fig. 1b via the dotted arrows. This elastokinematic effect allows the final stage to translate axially, further than allowed by pure axial compression [1,2,18]. The bearing performance with regards to the y-axis axial stiffness is thus compromised by the underconstraint. The flexural DP is often used as a bearing for microscale positioning stages driven by capacitive drives. It must resist pull-in effects via the DP axial stiffness (y-axis), over a range of displacements, so this large displacement axial stiffness reduction is of direct concern to device performance. This has been a common focus for bearing designers [3–6,14].

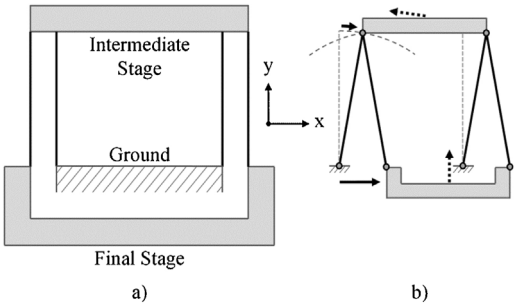

Fig. 1. a) Double parallelogram flexure bearing, with b) effective linkage model of the bearing undergoing displacement along its main translational DOF. The solid arrows show the main translation DOF motion, while the dotted arrows show the y-axis DOF of the final stage at large displacements enabled by the underconstrained DOF of the intermediate stage. Image from [1].

Please cite this article in press as: Panas RM. Large displacement behavior of double parallelogram flexure mechanisms with underconstraint eliminators. Precis Eng (2016), http://dx.doi.org/10.1016/j.precisioneng.2016.06.010